Petroleum and Coal

Article **Open Access**

Enhancing Casing Milling Performance through Mill Wear and Chip Type Prediction Using the Artificial Neural Networks (ANNs): Laboratory Experimental Case Study

Mohammed A. Namuq[1], Reda Abdel-Azim[1], Matthias Reich[2], Yibing Yu[3]*

[1] *Petroleum Engineering Department, Faculty of Engineering, The American University of Kurdistan, Zakho Road, 42001 Duhok, Iraq*

[2] *Institute of Petroleum Engineering, TU Bergakademie Freiberg, Agricolastr. 22, 09599 Freiberg, Germany*

[3] *School of Petroleum Engineering, Yangtze University, National Engineering Research Center for Oil & Gas Drilling and Completion Technology, Wuhan, China*

Received October 7, 2024; Accepted December 17, 2024

Abstract

The casing milling process of oil and gas wells is a crucial task and is widely applied during the side-tracking, abandonment operations of old wells, etc. Nevertheless, this process poses issues and problems, one of them being the safe and continuous removal of the produced chips from boreholes. Large fragments of the casing and long chip length, which lead to forming chip nests around the mill string, hinder the cleaning process of the borehole. Oppositely, short chip sizes do not pose previously mentioned issues. Another associated issue with milling processes is rapid mill wear and frequent replacement due to harsh working environmental conditions. Most of the efforts associated with the casing milling process in the literature are focusing on increasing the penetration rate, optimizing the milling tool design. The objective of this study is to develop a model using artificial neural networks (ANNs) for predicting the mill wear and the formed chip shape of metal casing milling processes. The operation parameters, mill rotation per minute and forward velocity (equivalent to penetration rate), were used as input parameters to train the ANNs. The target parameters are the produced chip shape of the metal casing string and the mill wear. In total, 72 data points collected from literature for the laboratory test rig simulating a wide range of practically reasonable casing milling operations were used for training and evaluating the model's effectiveness. The proposed ANNs model in this article was determined to be best for predicting the produced chip shape and insert wear for casing milling operations based on the highest coefficient of determination (R^2) between the measured and predicted values. The effectiveness of the model was evaluated by predicting the chip shape and insert wear of datasets, which were arbitrarily not included in developing the model. It can be concluded that the ANNs model is able to make predictions with a significantly higher R^2. The developed models are very promising and can be used to adapt the milling operation parameters to keep the milling process within the desired generated chip shapes and sizes, and reduce the wear on the mill. As a result, it will offer better borehole cleaning and removal of the chips, and will prevent the development of chip nests around the mill string and associated round trip costs and injury risks.

Keywords: *Oil/Gas well casing milling; Modeling casing milling operations; ANN application for casing milling; Optimizing the casing milling process.*

1. Introduction

Oil, gas and geothermal wells are drilled in sections; each section is secured by running a casing (string of steel pipes) and cementing it in place before drilling the next section. None-theless, for repairing, abandonment, or sidetracking purposes, casings need to be milled to small chips which are flushed out of the borehole by the drilling mud. Additionally, mature fields across the globe contain a significant amount of un-swept hydrocarbon reserves, which operators are increasingly making efforts to access and produce by utilizing sidetracking technology, a more economically viable option than traditional drilling [1]. The casing milling operations are full of challenges and pose issues. One of the common challenges is the growth of the so-called chip nests around the milling string due to producing long chips as shown in Fig. 1(b). This could restrict the annulus flow area and affect the chip removal in boreholes, and even can end up with the milling string getting stuck in the boreholes resulting in long-time fishing jobs. If a chip nest cannot be removed by a long flushing period, the entire drill pipe must be tripped out of the borehole to get the nest removed. The process of removing the sharp-edged chips from the drill pipe has a high injury risk [2-4]. In addition, due to the harsh working environment and unsuitable operation parameters for the milling tool, it can wear rapidly which ends up with a time-consuming round-trip for a milling tool replacement. Furthermore, if a piece of the casing breaks off before it is fully milled and properly processed as shown in the Fig. 1(a), it could lead to jamming in the borehole and can obstruct the drilling fluid circulation, which is supposed to carry the chips to the surface. Those issues in the milling process can prolong the non-productive time that leads to increased operational cost.

Namuq *et al.* found in their research study on casing milling operations in the laboratory that the operating parameters (mill RPM and forward velocity) have a significant influence on the generated chip shapes and sizes, as well as on the insert wear [3]. Murchie *et al.* stated that efficient milling requires an optimal bit design coupled with optimized milling parameters, for instance weight on mill, torque and RPM [5].

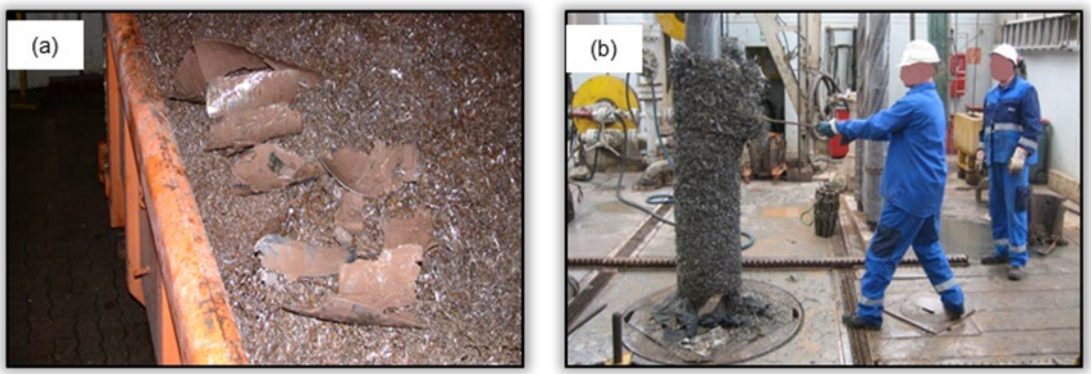

Fig. 1 (a) Casing fragments [source: EMPG], (b) Removal of a chip nest around a stabilizer [source RWE DEA], modified [3-4].

Stowe and Ponder claimed that savings of five days in average per well in the North Sea are achieved by carefully tailoring the cutter geometry and carbide chemistry to the downhole environment [6]. In 2012, Guidry and Thomas presented a method using inhouse-created drill-string dynamics finite element analysis (FEA) software for designing the milling BHA with the aim to reduce its operational bending stresses and to increase its fatigue life [7]. MacZura *et al.* presented the use of a memory sub for monitoring downhole forces applied when performing post frac milling operations to have a better understanding of the forces that are actually transmitted from the tools to the composite frac plugs in the actual wellbore environment [8]. Kocis *et al.* introduced the development and application of a technology based on electrical plasma for hard rock drilling and casing milling applications for well plug and abandonment operations [9]. Gajdos *et al.* also presented a milling technology which uses electrical plasma for material disintegration and claimed that the size distribution of cuttings produced during casing / tubing milling with the plasma-based tool is based on the major fraction in the range of 1-5 mm. This feature reduces the possibilities of intervention failures related to debris in the well [10].

An application of a hybrid section milling and under-reaming single-trip BHA with the aid of a time-based dynamic simulation system to remove a casing from the wellbore and under-ream the well to the virgin formation for an operator in The Netherlands was presented by

Wang *et al.*, in 2016 [11]. The dynamic simulation outcome was the creation of a pre-job planning roadmap to enable achieving the customer's Plug and Abandonment (P&A) objectives and ensuring the optimal utilization of each component of the single-trip BHA. Haq *et al.* presented and discussed the design optimization of a dual string section milling technology using CFD to eliminate wash out issues and erosion prone areas in the tool during field runs. They claimed that the development of this technology resulted significant time savings for the operators versus using conventional methods, in one offshore field case, it resulted in more than 20 days of savings in milling time [12]. In 2018, Nelson *et al.*, presented an approach for a 'swarfless' section milling system which mills a window in the casing by starting at the bottom of the interval and milling upwards the required length, mechanically moving and depositing the swarf in the rathole below. This approach was introduced as a solution for the key challenge faced when removing high volumes of casing while milling by circulating the generated steel cuttings/chips out of the well, and safely capturing and disposing them off [13].

Suppes *et al.* investigated the application of the well-known MSE (mechanical specific energy) concept for rock drilling to casing milling in an attempt to optimize the ROP [14]. Wiesenborn *et al.* highlighted design features of an automated wire line milling system. They claimed that the user can initiate the milling process by defining certain milling parameters. Then, the user can monitor progress in real time while the downhole robotic tool regulates the weight on bit and the milling motor [15]. Watson *et al*. introduced the deployment of a real-time downhole telemetry in milling operations in the Western Canadian Sedimentary Basin. Downhole telemetry was utilized to better understand motor performance, decrease motor damage and identify the key factors in lost circulation events [16]. Rosli *et al.* presented the advantage of a milling operation case via an electric line in challenging well environments. The electric line tractor conveyed the camera at high angles to successfully identify and mill the obstruction in the well [17]. Eslinger *et al.* presented a wellbore cleanup toolbox, claiming that it combines and optimizes the benefits of jetting, milling and chemical dissolution techniques. The system is used to clear obstructions from the wellbore [18]. Neema *et al.* presented a range of machine learning models which have been developed and evaluated using a training subset of field data from section-milling operations with main focus on improving the rate of penetration (ROP) in section-milling [19].

Yekta *et al.* showed that the real-time measurement of solids and flow rate monitoring enables the coiled tubing operator to make informed decisions throughout milling and cleanout operations. The acoustic monitor device is designed to measure the acoustic noise induced into the pipe wall as solids impact the inside wall of the pipe during milling operations. So, real-time solid measurement and return flow rate can be provided by utilizing the acoustic monitor and ultrasonic flow meter [20]. Zhou *et al.* developed a mathematical cutting model for hydraulic section milling operations and claimed that this study will serve as a theoretical basis for optimizing the structural and hydraulic parameters of hydraulic cutters and making further improvements in the cutting efficiency for the side-tracking and abandonment operations of old wells [21]. Noor *et al.* described the use of an electric line milling tool with a tractor and customized milling bit for a well in offshore East Malaysia which encountered a stuck wireline retrievable safety valve issue [22]. Fajardo *et al.* presented a coiled tubing milling operation case offshore at the coast of Louisiana showing that the combination of conventional milling techniques and real-time downhole measurement capabilities enabled rapid responses and adjustments to the actual downhole conditions throughout the operation. The real-time measurement was to remove common uncertainties that exist during coiled tubing operations including the question of whether the correct force was transmitted from the surface, the bottom hole assembly (BHA) was functioning correctly [23]. Namuq *et al.* presented the concept for developing measurement while milling system in real time by utilizing the accompanied acoustic emission signal to the casing milling process for determination of the formed chip class [4]. Elkasaby *et al.* presented an approach to improve the setting of a Whipstock followed by a window milling operation where the use of downhole weight, torque, bending moment, and 3-axis drillstring vibration measurements aimed to allow the drilling parameters to be constantly optimized without compromising the integrity of the downhole tools in an

Offshore Field in Norway. The positive-pulse telemetry system that was configured for a wide range of downhole flow and mud-weight conditions performed flawlessly across the complex operation with almost 100% data detection efficiency [24].

Most of previously mentioned studies tackled the hardware part of the milling tool to increase ROP, coupling the milling process with a real time monitoring system, in order to overcome or mitigate the challenges faced in the milling process. According to the available literature, there is no model focused on enhancing the milling process through forecasting the mill wear and/or the formed chip type. This research work concentrates on developing a model using ANNs to predict the chip class and insert wear under specific operation conditions. The available data in the literature for a laboratory experiment at the Technical University Bergakademie Freiberg in Germany has been used to train and validate the developed model. The data set simulates a wide range of the milling process. A good correlation has been found between the model prediction and those measured data in the lab with an R^2 of more than 90%. The model can serve as a tool for engineers seeking to determine operation parameters where the desirable range of chip types and mill wear will be expected for the milling process, as a result, achieving a continuous removal of the chips and minimizing round-trips. Furthermore, using of the proposed new model is very cost-effective in terms of reducing the number of experiments conducted.

2. Case study: laboratory experimental test

2.1. Lab description

The available data set in the literature for the small-scale model casing milling test rig equipped with sophisticated measurement technology at the Institute of Drilling Engineering and Fluid Mining (IBF) of the Technical University Bergakademie Freiberg in Germany has been utilized for developing and testing the model. In this article, the laboratory experiment for the casing milling will be only shortly described, the reader is referred to the references [3-4,25] for more details of the test rig, conducted experiments, etc. The main aim of the test rig was to investigate and conduct basic research on the casing milling process in boreholes, see the Fig. 2.

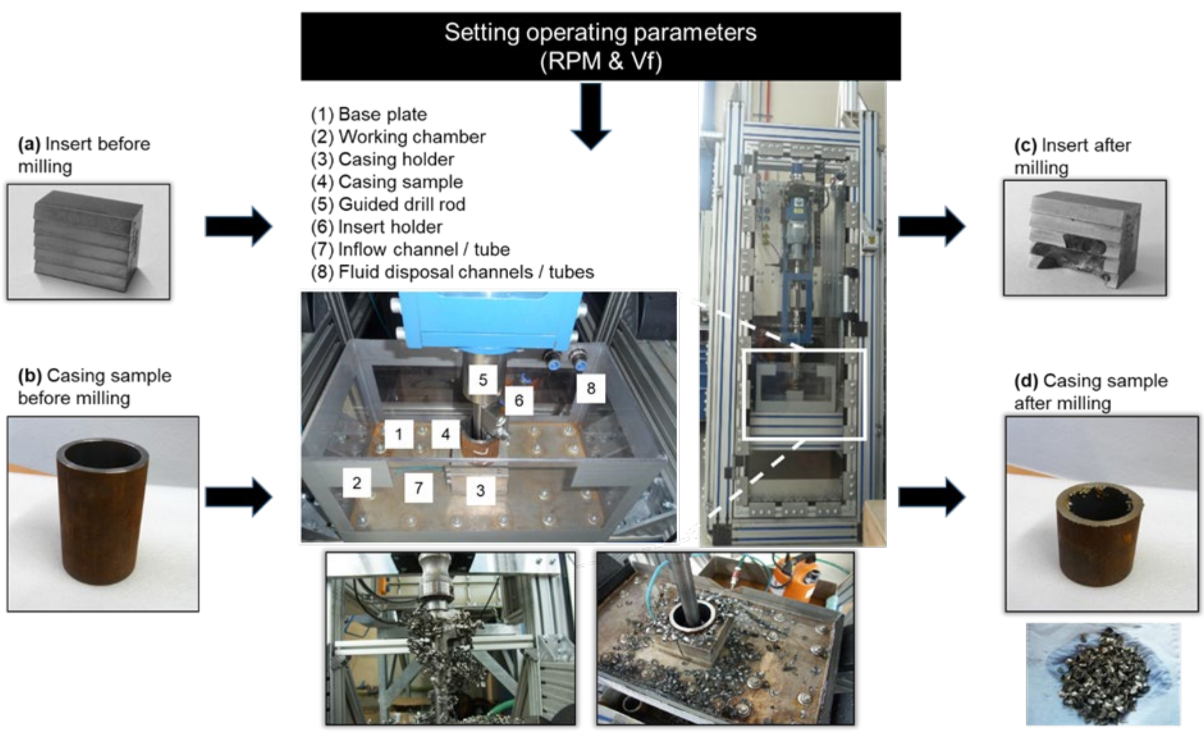

Fig. 2. Small scale test rig for performing casing milling test, (modified [3-4,25]).

The base plate (1) in the Fig. 2 is fixed to the lower side of the working chamber (2), this enables the collection of the produced chippings. The individual casing holder (3) is drafted and designed for each individual casing to fit the outside diameter (for instance; 48.26, 60.325, 73.025 and 88.9 mm). The used cooling fluid (water) for the casing milling process flows through a tube (7), specifically, from the bottom of the working chamber into the casing sample (4) and leaves the working chamber through tubes (8). The insert holder (6) holds one insert. The advantage of a single bladed tool is that a defined contact of the insert with the chipping surface permanently exists. In order to use the insert holder (6) for different casing dimensions and wall thicknesses, an adapter or spacer is mounted between the insert holder (6) and the drilling rod (5) [3-4]. The inserts are held by a clamping and screw system, which is similar to common machines used in the metal processing industry. This provides easy access for mounting and/or replacement.

2.2. Test data

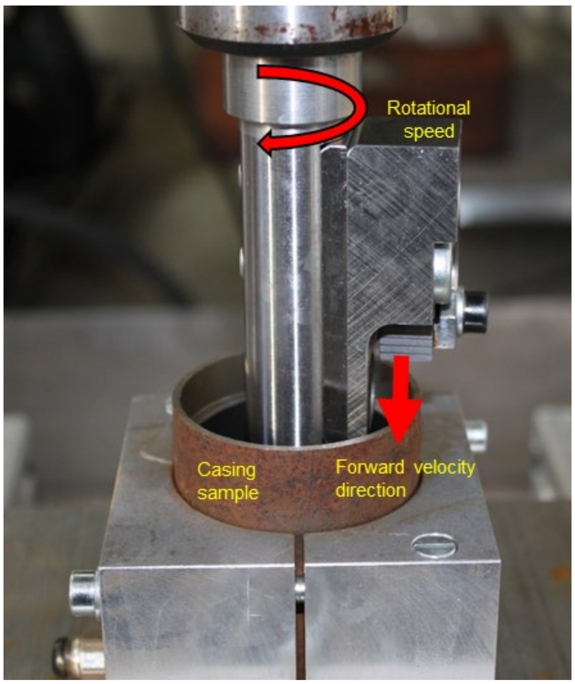

Fig. 3 The operating parameters for the casing milling process [3].

The available 72 test points have been collected from the literatures [3-4,25], which simulate wide range of milling process conditions. The data were gained at different rotational speeds, which ranged from 40 to 370 rpm, and different forward velocities between 0.04 mm/s and 0.4 mm/s (0.144 m/h to 1.44 m/h), see the Fig. 3 for explanation about the setting parameters of the casing milling test.

For all collected test points, the type of insert is kept constant, see Fig. 2 (a). Likewise, the casing type, L80 with OD of 60.325 mm, is also kept the same for all performed tests. Before conducting a test, the casing sample was prepared in pieces of approximately 100 mm in length as shown in the Fig. 2 (b). For each test, new casings and inserts were used. The inserts were weighed before and after each test and the volume of milled casing was determined. The figure 2 (a, b, c, d) shows the insert and casing sample before and after the milling test. For each test the forward velocity and RPM were set to specific values.

The chip type for each performed test was determined according to the table below which shows the existing chip shape classification starting from 1 (critical) to 8 (very preferred). Fig. 2, middle on the left side shows one of the tests with critical produced chips. In contrast, in the middle, on the right side the picture shows preferred produced chips achieved with another test.

Table 2 below includes the test points which were used for developing and validating the ANNs model. Only chip shape class for 5 test points (66 to 70) were not available and documented in the available literature, therefore they left empty in the table below.

Table 1. Chip shape classifications according to Denkena and Tönshoff, (modified [26])

Chip name	Chip shape	Chip shape classification	Rating
Ribbon chip		1	Critical
Snarled chip		2	Critical
Helical chip		3	Critical
Cylindrical helical chip		4	Not preferred
Discontinuous helical chip		5	Preferred
Spiral chip		6	Preferred
Discontinuous spiral chip		7	Very preferred
Discontinuous chip		8	Very preferred

Table 2. Test data of the milling process for the laboratory case study, (modified [3-4,25]).

Test point	Rotational speed	Vf (forward velocity)	Chip shape class	insert wear (in gm of insert per drilled casing volume in m^3)
No	rpm	mm/s	Unitless	gm/m^3
1	40	0.05	6	2161
2	75	0.05	6	1410
3	75	0.1	6	3071
4	75	0.15	6	6953
5	75	0.2	6	5576
6	110	0.05	6	2102
7	110	0.1	6	3471
8	110	0.2	5	4452
9	110	0.3	7	3814
10	110	0.35	7	4884
11	110	0.4	7	5798
12	110	0.15	5	4417
13	110	0.25	7	6689
14	110	0.05	6	1811
15	175	0.05	3	12
16	175	0.1	4	2224
17	175	0.15	5	3959
18	175	0.2	7	2916
19	175	0.25	7	8930
20	175	0.3	7	6763
21	370	0.05	2	90
22	40	0.05	6	2512
23	75	0.1	6	5687
24	75	0.15	6	5975
25	75	0.05	6	4289
26	75	0.2	7	13258

Test point	Rotational speed	Vf (forward velocity)	Chip shape class	insert wear (in gm of insert per drilled casing volume in m^3)
27	110	0.05	7	3280
28	110	0.15	7	5440
29	110	0.1	8	14925
30	110	0.2	7	9357
31	175	0.15	6	3364
32	175	0.2	5	4467
33	175	0.1	8	6023
34	175	0.05	8	2219
35	175	0.05	8	3582
36	175	0.1	7	2629
37	175	0.15	7	6696
38	100	0.16	8	5478
39	100	0.14	8	11110
40	100	0.12	8	9113
41	100	0.1	7	15981
42	100	0.08	8	9379
43	100	0.06	8	3503
44	100	0.04	8	2639
45	125	0.16	8	11040
46	125	0.14	8	14652
47	125	0.12	7	8739
48	125	0.1	8	25799
49	125	0.08	8	5220
50	125	0.06	8	5023
51	125	0.04	8	2651
52	150	0.16	7	3466
53	150	0.14	7	3384
54	150	0.12	6	2060
55	150	0.1	7	1832
56	150	0.08	7	3137
57	150	0.06	8	142
58	150	0.04	8	6385
59	175	0.16	7	5631
60	175	0.14	8	10017
61	175	0.12	8	6253
62	175	0.1	8	4653
63	175	0.08	8	4704
64	175	0.06	8	3887
65	175	0.04	8	2332
66	200	0.12		2972
67	200	0.1		5524
68	200	0.08		10145
69	200	0.06		6466
70	200	0.04		13121
71	370	0.4	8	25799
72	40	0.04	2	12

3. ANNs model and results

A wide range of machine learning algorithms have been applied to predict various petroleum engineering properties, including neural networks (ANN), random forests (RF), function networks (FNs), adaptive neuro-fuzzy inference systems (ANFIS), and support vector machines (SVM). Some researchers have combined different machine learning algorithms or incorporated additional techniques (e.g., calibrated bias) to enhance prediction accuracy [27-31].

Backpropagation is a supervised learning algorithm commonly used in artificial neural networks (ANNs). This is a method of training the network by adjusting its weights and biases to minimize the error between the predicted output and the actual target output. The quadratic cost function is a popular choice for measuring the error between the predicted and actual outputs. It is defined as follows:

$$J(w, b) = 1/2n * \Sigma(\hat{y} - y)^2 \qquad (1)$$

whereby: J(w, b) is the cost function; n is the number of training examples; y^ is the predicted output; y is the actual output.

The cost function calculates the average squared difference between the predicted and actual outputs. By minimizing this cost function, the network learns to produce more accurate predictions.

Backpropagation process includes:

1. **Forward propagation:**
   - Input data is presented to the network.
   - The input is propagated through the hidden layers and finally to the output layer.
   - The network produces a predicted output.
2. **Error calculation:**
   - The difference between the predicted output and the actual target output is calculated using the cost function.
3. **Backward propagation:**
   - The error is propagated backward through the network, starting from the output layer and moving to the hidden layers.
   - At each layer, the error is used to calculate the gradient of the cost function with respect to the weights and biases.
4. **Weight and bias update:**
   - The weights and biases are updated using gradient descent, adjusting them in the direction that minimizes the cost function.

A gradient descent method was used in this study to optimize neural network performance by modifying the connection weights and computing the delta weight vector to minimize the cost function. In this study, a stopping criterion has been employed in the Artificial Neural Network (ANN) based on a fixed error threshold, a fixed number of allowable epochs, and the use of validation data. These criteria are highly sensitive to input parameters, and improper selection can lead to poor performance due to excessive training. Notably, the target output during training is typically scaled within the interval of 0 and 1 for the logistic function. During the learning phase, it is crucial to test the neural net's performance at each epoch. Therefore, we utilize the mean square error (MSE) as shown in Equation 2 to evaluate network performance.

$$MSE = \sqrt{\frac{\sum_1^{n1}\sum_1^{n2}\left(x_p - y_p\right)}{n_1.n_2}} \qquad (2)$$

where: n1, n2 are number of training output neurons respectively; xp and yp are the target and calculated outputs, respectively.

In this study, we used 72 data points to train and test the ANN model. The data set includes two crucial inputs: mill RPM and forward velocity as shown in Table 3. The output of the model is milling wear.

Table 3. Statistics analysis of the input data.

Parameter	Mill RPM	Vf (forward velocity)
Max	370 rpm	0.4 mm/s
Min	40 rpm	0.04 mm/s
Standard deviation	49.832	0.0754
Skewness	1.776	1.5459
Mean	125	0.1

The data set was divided into 70% for training and 30% for testing. The back propagation learning algorithm is used to minimize the error between actual and target outputs using the log sigmoid function. The results were exceptional, with an R^2 of 0.93 and MSE = 0.018 for training, see Figure 4, and an R^2 of 0.96 for testing, see Figure 5. In addition, a mathematical correlation was produced, enabling the forecasting of milling wear using the aforementioned inputs.

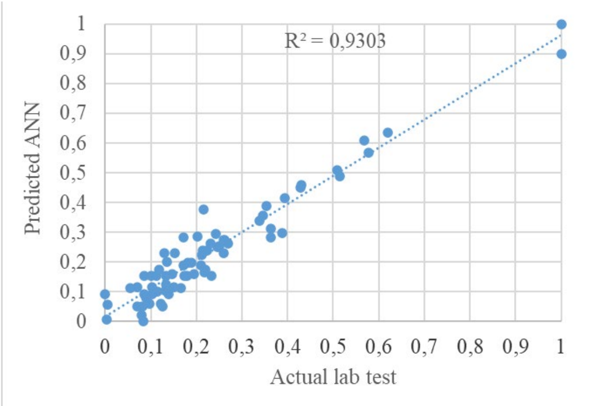

Fig. 4. The predicted drilling insert wear from ANN versus actual lab test data for training.

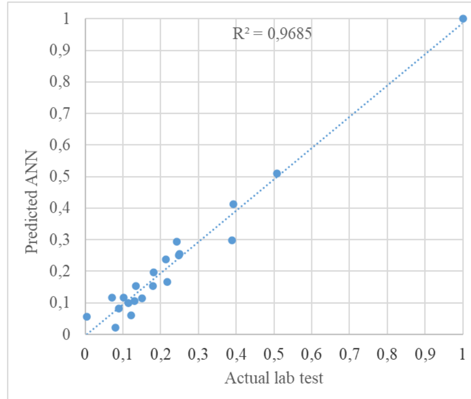

Fig. 5. The predicted drilling insert wear from ANN versus actual lab test data for testing.

The novel correlation generated using ANN for milling wear estimation is given by:

$$Wmn = \left[\sum_{i=1}^{N} w_{2i} \operatorname{tansig}\left(\sum_{J=1}^{J} w_{1i,j} x_j + b_{1j} \right) \right] + b_2 \qquad (3)$$

$$Wmn = \left[\sum_{i=1}^{N} w_{2i} \left(\frac{1}{1 + exp^{-\left(RPM \times w_{1,j,1} + Forward-Velocity \times w_{1,j,2}\right) + b1}} \right) \right] + b_2 \qquad (4)$$

where: W_{mn} is the normalized milling wear; ($w_{2,i}$) is the vector weight between the hidden layer and the output layer; ($w_{1,j}$) is the vector weight connecting the input and the hidden layer; j is the neuron number; b_1 is the biases vector for the input layer; and b_2 for the output layer, x is the input values.

The extracted insert wear equation can be attained by de-normalizing W_{mn} as follows:

$$Wear - Mill = 25790 \times Wmn + 12.433 \qquad (5)$$

Table 4 shows the weights and bias for the correlation. The proposed correlation in equations 3, 4 and 5 can be used to estimate and predict the insert wear in gm per drilled casing volume in m^3 using the above-mentioned inputs.

Table 4. Weights and biases for the generated correlation Eq. (3, 4 and 5).

Rotation per minute	Vf (forward velocity)	Hidden and output layers weights	Hidden layer bias (b1)	Output layer bias (b2)
W1		*w2*	*b1*	*b2*
0.0307	-3.4453	-1.0886	2.73317	0.27389
21.9378	16.1124	-14.545	-11.326	
-1.2504	-0.4627	-3.1987	0.79832	
-46.928	6.75571	7.38495	9.43607	
-8.4139	1.60616	-5.8863	3.57852	
-4.8563	0.82555	-4.3792	1.27401	
15.3817	47.4797	-13.202	24.7092	
-9.2422	-2.5325	6.6107	8.01124	
0.8409	12.9918	-5.8855	13.1274	
-22.925	12.7625	0.30938	-14.686	
-34.977	-18.814	3.45447	-16.771	
-37.696	-64.291	23.2134	9.36253	
-11.905	2.31116	-6.4949	5.06238	
-4.8606	19.8963	-13.396	17.3902	

Rotation per minute	Vf (forward velocity)	Hidden and output layers weights	Hidden layer bias (b1)	Output layer bias (b2)
W1		*w2*	*b1*	*b2*
-3.7139	0.73301	-3.627	0.36721	
89.1112	12.4903	-28.517	-22.84	
18.4229	92.3271	-22.266	-13.525	
-62.948	-5.0946	18.82	-21.753	
26.689	3.97058	-11.449	6.79291	
0.01582	0.62088	-3.187	-0.6104	

The correlation, as shown in equations 3, 4 and 5, demonstrates that the designed ANN model is reliable and significantly reduces computational time compared to traditional numerical simulation models that require extensive mathematical knowledge. Table 4 provides the weights and bias for the correlation, and Figure 5 illustrates the excellent matching between the actual milling wear and the values extracted from the ANN model. This ANN model could offer substantial benefits in optimizing milling wear and enhancing computational efficiency.

Furthermore, an ANN model has been also developed to predict the chip shape. The novel correlation generated using ANN for chip shape estimation is given by:

$$Chip-norm=\left[\sum_{i=1}^{N} w_{2i}\,\text{tansig}\left(\sum_{J=1}^{J} w_{1i,j}x_j+b_{1j}\right)\right]+b_2 \qquad (6)$$

$$Chip-norm=\left[\sum_{i=1}^{N} w_{2i}\left(\frac{1}{1+exp^{-\left(RPM\times w_{1,j,1}+Forward-Velocity\times w_{1,j,2}\right)+b1}}\right)\right]+b_2 \qquad (7)$$

Where Chip-norm is the normalized chip shape, (w2, i) is the vector weight between the hidden layer and output layer. (w1, j) is the vector weight connecting the input and the hidden layer, j is the neuron number, b1 is the biases vector for the input layer, and b2 for the output layer. Table 5 shows the weights and bias for the above correlations. The extracted chip shape equation can be attained by de-normalizing chip-norm as follows:

$$Chip-shape=6\times Chip-norm+2 \qquad (8)$$

Table 5. Weights and biases for the generated correlation Eq. (6, 7 and 8).

Rotation per minute	Vf (forward velocity)	Hidden and output layers weights	Hidden layer bias (b1)	Output layer bias (b2)
W1		b_1	w_2	b_2
1.067794	20.72991	-1.41183	17.35977	-0.83748
34.93764	8.866616	-1.18537	26.05825	
-0.59949	36.95645	28.85683	18.26031	
-29.4868	4.465693	6.73186	-26.5945	
-1.21313	-28.3498	0.321753	-6.91178	
9.710554	-4.97784	1.135307	13.25349	
0.15881	-5.59526	-17.0261	-7.91511	
41.58512	-7.37958	23.99665	3.026729	
3.375249	-9.19744	-2.32869	13.12735	
-26.6029	-1.04889	-2.54007	-14.686	
1.984726	16.06158	-12.1216	-16.771	
-67.6983	16.85338	-1.65786	0.467006	
-3.27818	-4.20627	-4.81345	-27.6535	
3.268706	-6.75702	-19.79	-13.8914	
-2.90143	-15.7157	3.488522	-0.7415	
12.40072	-3.55453	-6.70464	-1.78684	
1.523479	0.164731	7.868523	12.11216	
26.65986	0.186135	-27.5616	7.670017	
-0.31873	5.933706	-10.1037	-0.16084	
12.40702	27.52302	32.66082	0.837634	

The ANN model successfully predicted the chip shape with a high accuracy, as demonstrated by the R^2 values of 0.968 for training and 0.962 for testing. The Figures 6 and 7 likely provide visual comparisons between the predicted and actual chip shapes, further confirming the model's accuracy. The ability to accurately predict chip shapes using an ANN model could be valuable for enhancing the casing milling process and mitigating the issues associated with generating non-preferred chip shapes.

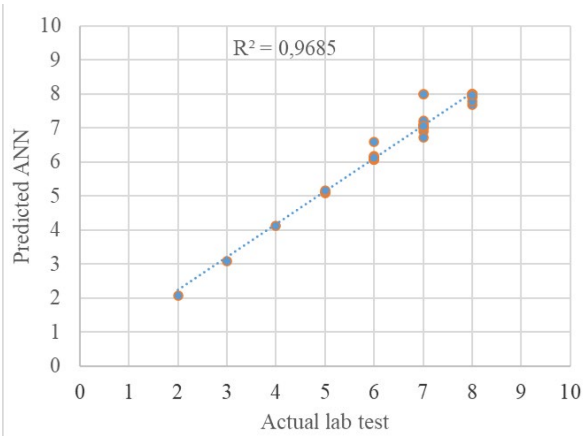

Fig. 6. The predicted chip shape from ANN versus actual lab test data for training.

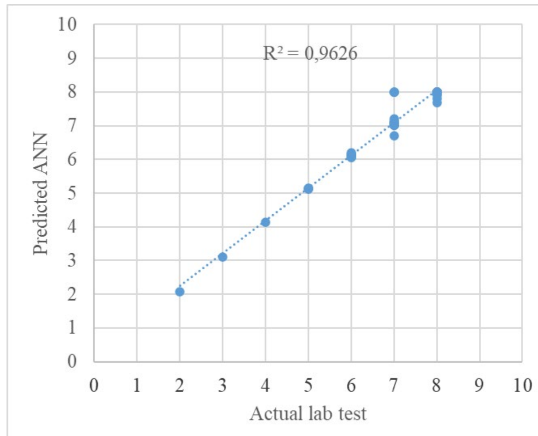

Fig. 7 The predicted chip shape from ANN versus actual lab test data for testing.

4. Conclusions and recommendations

In this study, a model has been successfully developed using Artificial Neural Networks (ANNs) for predicting insert wear and chip shape class for the casing milling process with an attempt to tackle the challenges in the milling process. As a result, the overall casing milling performance is enhanced. The available lab test data for the exceptionally developed small-scale laboratory prototype were used to train and also validate the effectiveness of the model. The model forecasting is in good agreement and correlation for those performed lab tests with the highest coefficient of determination (>90%) between the measured and predicted chip shape class and insert wear.

The results and findings of the use of ANNs model are very encouraging. It seems that pre-job predictable milling operations could be achieved through predicting the chip shape class and insert wear to work in the less challenging operation range. Therefore, it can be concluded that it is quite a viable and promising idea to have a pre-job adjustment for the operation parameters in order to avoid rapid mill tool wear, challenges with chip removal, blocking the circulation, and frequent round-trips.

Due to the complexity of the milling process, it can, therefore, be suggested that further studies are required to cover wider milling operation conditions, even field cases, and to safely and thoroughly validate the existing findings. Such models will help in making pre-job decisions and in providing clear guidelines for practical applications of the milling process, hence adapting the operation parameters accordingly.

Acknowledgments

We would like to express our deep thanks to the DGMK (Deutsche Wissenschaftliche Gesellschaft für Erdöl, Erdgas und Kohle e.V.) for funding the first phase of the project to setup the modern milling test rig. Furthermore, we express our thanks to Dr. Ezideen Ali Hasso for reading the article and his comments.

Abbreviations

ANNs	*Artificial Neural Networks*	V_f	*Forward velocity*
RPM	*Rotation per minute*	*OD*	*Outside diameter*

References

[1] Chukwuemeka AO, Afolabi PO, Ibegbule SO, Oluro AB. Lowering cost and improving the production efficiency of sidetrack wells in mature fields. Petroleum and Coal Journal, 2017; 59(3): 327-338.

[2] Karsch H. Eine Herausforderung: über 800 m 13 3/8" Rohre fräsen. DGMK/ÖGEW- Frühjahrstagung 2014, Fachbereich Aufsuchung und Gewinnung Celle, Celle, Germany, 2014.

[3] Namuq MA, Berro MJ, Reich M. Investigating the effects of operating parameters on the increase of the casing milling efficiency in deep drilling operations. Oil Gas European Magazine, 2019; (2): 55–61.

[4] Namuq MA, Berro MJ, Reich M. Measurement-While-Milling (MWM): An innovative approach for increasing the casing milling efficiency in deep drilling operations. Petroleum Research Journal, September 21, 2022; 8(3): 360-369.

[5] Murchie S, McInally G, Tinnen B, Gabriel K. Electrohydraulic Tractor and Associated Mechanical Technology Platform Developments Deliver Precise, Controlled and Highly Effective Capability for Efficient Completion Component Milling. Paper presented at the SPE/ICoTA Well Intervention Conference and Exhibition, The Woodlands, Texas, USA, March 16, 2020: SPE-199809-MS.

[6] Stowe C., Ponder A. Performance advance in section milling technology. Paper presented at the SPE Annual Technical Conference and Exhibition, Denver, Colorado, USA, October 30, 2011: SPE-145957-MS.

[7] Guidry CW, Thomas R. Innovative Casing Exit Milling System Optimized Using Drillstring Dynamics Simulation for Efficient Multilateral Completions. Paper presented at the IADC/SPE Asia Pacific Drilling Technology Conference and Exhibition, Tianjin, China, July 9, 2012: SPE-156477-MS.

[8] MacZura JM, Miller M, Scuadroni N, Daley D. Effects of downhole parameters on horizontal milling applications. Paper presented at the SPE Annual Technical Conference and Exhibition, Houston, Texas, USA, September 28, 2015: SPE-174921-MS.

[9] Kocis I, Kristofic T, Gajdos M, Horvath G, Jankovic S. Utilization of electrical plasma for hard rock drilling and casing milling. Paper presented at the SPE/IADC Drilling Conference and Exhibition, London, England, UK, March 17, 2015: SPE-173016-MS.

[10] Gajdos M, Mostenicky I, Kocis I, Kristofic T, Plichta M, el Bannan G, Taha I. Plasma-based milling tool for light well intervention. Paper presented at the SPE/IADC Middle East Drilling Technology Conference and Exhibition, Abu Dhabi, UAE, January 26, 2016: SPE-178179-MS.

[11] Wang Y, Vos M, Karimpour A, Fearn M, den Besten H, Stanko T, Bain J, Shen Y, Stokes D, Issa A, Khan Z. Integration of Time-Based Dynamics Simulation with Milling and Underreaming System to Implement Reliable Single Trip Solution in Plug and Abandonment Operation. Paper presented at the IADC/SPE Drilling Conference and Exhibition, Fort Worth, Texas, USA, March 1, 2016: SPE-178866-MS.

[12] Haq M, Deshpande K, Imtiaz K, Smalley M. Optimization of Design Using Computational Fluid Dynamics Technique for New P&A Down Hole Milling Technology - Case Studies of Rig Run Comparisons Validating Design Changes. Paper presented at the Abu Dhabi International Petroleum Exhibition & Conference, Abu Dhabi, UAE, November 12, 2018: SPE-192935-MS.

[13] Nelson JF, Jørpeland J, Schwartze C. Case History: A New Approach to Section Milling: Leaving the Swarf Behind!. Paper presented at the Offshore Technology Conference, Houston, Texas, USA, April 30, 2018: OTC-28757-MS.

[14] Suppes R, Ebrahimi R, Krampe J. Optimising casing milling Rate Of Penetration (ROP) by applying the concept of Mechanical Specific Energy (MSE): a justification of the concept's applicability by literature review and a pilot study. Elsevier, Journal of Petroleum Science and Engineering, September 2019; 180: 918-931.

[15] Wiesenborn K, Baklanov N, Gourmelon PO, Klyushev M, Yang X. Automated wireline milling system. Paper presented at the SPE/ICoTA Well Intervention Conference and Exhibition, The Woodlands, Texas, USA, March 18, 2019: SPE-194232-MS.

[16] Watson B, Layton B, Matiasz K. Optimized milling and intervention operations in low pressure wells by combining real-time downhole telemetry and diverting agents. Paper presented at the SPE/ICoTA Well Intervention Conference and Exhibition, The Woodlands, Texas, USA, March 16, 2020: SPE-199857-MS.

[17] Rosli AF, Md Noor AS, Foo NK, Jelie A, Salleh FA, Omar MZ, Sulhi AH. World’s first EGF Flapper milling via E-Line. Paper presented at the SPE/ICoTA Well Intervention Conference and Exhibition, The Woodlands, Texas, USA, March 16, 2020: SPE-199861-MS.

[18] Eslinger D, Johnson AB, Mcdonough A, Oettli M. A hybrid milling/jetting tool – The safe solution to scale milling. Paper presented at the SPE/ICoTA Coiled Tubing Roundtable, Houston, Texas, April 5, 2000: SPE-60700-MS.

[19] Neema S, Singh L, Chiquiza F, First J, Collier C, Oo T, Katla K, Martin D. Data-Driven Performance Optimization in Section Milling. Paper presented at the Offshore Technology Conference, Virtual and Houston, Texas, August 9, 2021: OTC-30936-MS.

[20] Yekta K, Phung R, Stang B, Woitas T. Application of real-time solid measurement and return flow rate during coiled tubing milling operations. Paper presented at the SPE/ICoTA Well Intervention Conference and Exhibition, Virtual, March 15, 2021: SPE-204451-MS.

[21] Zhou X, He S, Tang M, Li Y, Zhang G, Liu X. Structural design and mathematical cutting model of hydraulic section milling for high-strength casings in small wellbores. Elsevier, Journal of Petroleum Science and Engineering, November 2022; 218: 111044.

[22] Noor ASM, Abdul Ghani SA, Panichakul P, Azman A, Atim FA. Wireline retrievable safety valve E-line milling. Paper presented at the SPE/ICoTA Well Intervention Conference and Exhibition, The Woodlands, Texas, USA, March 15, 2022: SPE-208995-MS.

[23] Fajardo SR, Adams E, Williams C. Downhole coiled tubing telemetry reduced time and uncertainty during a challenging deep water milling operation. Paper presented at the SPE/ICoTA Well Intervention Conference and Exhibition, The Woodlands, Texas, USA, March 15, 2022: SPE-209001-MS.

[24] Elkasaby S, Parker T, Munoz D, Slettebo E. A Novel Approach to Improve Whipstock Setting and Milling Operations with Existing Downhole Measurement and Logging Technology in an Offshore Field, Norway. Paper presented at the ADIPEC, Abu Dhabi, UAE, October 2, 2023: SPE-216250-MS.

[25] Namuq MA, Berro MJ, Klein S, Jordanow N, Schubert M, Reich M. Investigation on the improvement in efficiency of milling applications in drilling engineering. Final report, Deutsche Wissenschaftliche Gesellschaft für Erdöl, Erdgas und Kohle, Hamburg, 2018.

[26] Denkena B, Tönshoff HK. Spanen: Grundlagen. Springer, 2011.

[27] Abdel Azim R, Hamada G. Novel correlation for calculating water saturation in shaly sandstone reservoirs using artificial intelligence: Case study from Egyptian oil fields. ACS omega, August 16, 2022; 7(34): 29666-29674.

[28] Azim RA. Estimation of fracture network properties from FMI and conventional well logs data using artificial neural network. Upstream Oil and Gas Technology, September 2021; 7: 100044.

[29] Azim RA. Prediction of multiphase flow rate for artificially flowing wells using rigorous artificial neural network technique. Flow Measurement and Instrumentation, December 2020; 76: 101835.

[30] Fulford DS, Bowie B, Berry ME, Bowen B, Turk DW. Machine learning as a reliable technology for evaluating time/rate performance of unconventional wells. SPE Economics & Management, January 27, 2016; 8(01):.23-39.

[31] Klie H. Physics-based and data-driven surrogates for production forecasting. Paper presented at the SPE Reservoir Simulation Symposium, Houston, Texas, USA, February 23, 2015: SPE-173206-MS.

To whom correspondence should be addressed: Mohammed A. Namuq, Petroleum Engineering Department, Faculty of Engineering, The American University of Kurdistan, Zakho Road, 42001 Duhok, Iraq,
E-mail: mohammed.namuq@auk.edu.krd